

Article

A Technique for Optimizing the Sequences Yielding under Load of Concentrically-Braced Steel Frames

Bin Li ¹, Zhan Wang ¹, Yanjing Fan ¹, Jianrong Pan ^{1,*} and Zhenfeng Zhou ¹

¹ State Key Laboratory of Subtropical Building Science, South China University of Technology, Guangzhou 510640, China

² Department of Civil Engineering, Dongguan University of Technology, Dongguan 523808, China

* Correspondence: ctjrpan@scut.edu.cn

Abstract: Concentrically-braced steel framing is widely used in tall buildings. Designing with adequate but not excessive seismic resistance is a challenge because of the limited experience of seismic failure and the huge variety of components used. A quantitative method for defining an acceptable range of component parameters is proposed and tested using published experimental data and finite element modeling. The method involves the structural yield mechanism control method of the steel concentrically-braced frame. It is proposed by inequality iteration of different structural components' bearing capacities. It generates acceptable ranges for the parameters defining the properties of the columns, beams, and braces. The test results show that concentrically-braced steel frames designed within the recommended ranges will have the desired sequence of component yielding. The sequence is, however, highly sensitive to components' parameter values. In practical engineering stochastic variability in the parameters must be considered.

Keywords: concentric bracing; steel frames; yield mechanism control; component parameters; finite element analysis



Citation: Li, B.; Wang, Z.; Fan, Y.; Pan, J.; Wang, P.; Zhou, Z. A Technique for Optimizing the Sequences Yielding under Load of Concentrically-Braced Steel Frames. *Buildings* **2022**, *12*, 1656. <https://doi.org/10.3390/buildings12101656>

Academic Editors: Lulu Zhang, Peijun Wang, Zhe Xing and Boshan Chen

Received: 21 September 2022

Accepted: 9 October 2022

Published: 11 October 2022

Publisher's Note: MDPI stays neutral with regard to jurisdictional claims in published maps and institutional affiliations.



Copyright: © 2022 by the authors. Licensee MDPI, Basel, Switzerland. This article is an open access article distributed under the terms and conditions of the Creative Commons Attribution (CC BY) license (<https://creativecommons.org/licenses/by/4.0/>).

1. Introduction

Steel frames with concentric bracing are widely used in engineering practice due to their relatively light weight, good lateral resistance, and excellent seismic performance. With well-designed bracing, a structure's horizontal displacement can be effectively reduced, and the internal forces on the structural components can be more effectively distributed.

Today, designing such structures requires the designer to select the initial component sections based on experience, check the structural constraints, and finally complete the scheme. However, the braces are invariably designed too large or too small with any one designer's limited experience. If so, the structure's seismic resistance and also its economics will be sub-optimal [1]. In an earthquake, either the beams or the columns will yield first. But even if the structure has excellent energy dissipation capacity and safety performance it is still necessary to understand the sequence in which structural components will yield.

The Chinese standards GB50011-2010 [2] and GB50017-2017 [3] for the design of concentrically-braced steel frames, like the current EN1998-1 (also referred to as EC8 [4]), and the American AISC341-16 [5] standards, require consideration of the yield sequence of the structural components, and the braces should yield first. Meanwhile, many experimental, numerical and post-disaster field investigations (e.g., [6]) have demonstrated that larger brace sections can be designed by the internal force amplification method and that braces stronger than the other structural components will lead to larger responses to seismic excitation. That results in a structure's poor ductility. However, braces that are too small will impair a structure's seismic performance, energy dissipation capacity, and lateral stability. Research has shown that the mechanical properties of bracing are affected by the slenderness ratios [7,8], the width-thickness ratios [9], and the boundary constraints [10].

Reasonable slenderness ratio values have been suggested, but the current design methods do not control the yield sequence of a structure's components which can lead to inefficient and unreliable structures.

In recent years, the structural plasticity design method has received much research attention, and controlling yield mechanisms is a key problem to be solved. The method is based on energy balances [11–14], and it ensures that any plastic hinges are located at beam ends. Initially, however, the method did not consider the influence of stiffness and strength degradation in response to loading a structure. That can lead to unpredicted failure of a structure's components. To solve this problem, a hysteretic energy correction coefficient was introduced into the method [15], generating a more accurate equilibrium capacity plastic design. Otherwise, the plastic design methods for eccentrically braced steel frames [16], frames with X-concentric braces [17], and frames with V-concentric braces [18] can work with just a coefficient for the allowable dynamic horizontal force [19] and predict the expected failure mode, which can be adjusted by adjusting the columns. If the designer also wants to consider yield control for a structure's components, the plastic method is difficult to implement, and it is necessary to clarify the relationship between the structural components' parameters and the yield mechanism.

In this work, a method for optimizing concentrically-braced steel framing with yield mechanism control was developed and tested. The relationships of the parameters of a structure's different components with the structure's yield mechanism were studied. The range of component parameters used in the bending bearing strength calculations under the structure's yield criterion was obtained by using the inequality recursive iteration method, and a yield control mechanism was proposed. The proposed method was demonstrated to provide a theoretical basis for efficient optimization.

2. Yield Mechanism Control Method

Failure of a concentrically-braced steel frame typically involves the buckling failure of the braces in compression and tension, yielding failure of the braces' joint plate, and/or yielding of the beams and columns. Different patterns of component yielding significantly influence a structure's mechanical performance and ductility. Table 1 summarizes the design specifications applied in China, the US, and the EU and also some research results on yield mechanism control. All design suggestions specify that the braces should yield before the beams, and the beams should yield before the columns. The control criteria studied in this work were *strong column-weak beam* and *strong column and beam-weak brace*.

Table 1. Suggestions on structural yield mechanism control in References and specifications.

References and Specifications	Suggestions on Structural Yield Mechanism Control
GB 50017 [2]	Braces yield before beams and columns yield
GB 50011 [3]	The beams remain elastic when braces yield
AISC-341 [4]	The braces should yield first
EC8 [5]	The bearing capacity of beams and columns after the braces yield should be checked
Roeder, Lehman & Yoo [20]	The energy dissipation capacity of the braces should be fully utilized to ensure that the braces yield before the beams and column

In this work, a structure's yield mechanism was controlled using d (the inner diameter of a brace), D (the external diameter of a brace), w_{cf} (the width of the column's flanges), and $h_{cw}t_{cw}$ (the cross-sectional area of column's webs) assuming tubular braces, as shown in Figure 1. Those parameters were defined iteratively using an inequality representing the structure's bending bearing capacity. For braces that are not tubular, the bending yield strength calculations need to be modified, but the inequality iteration will not be changed.

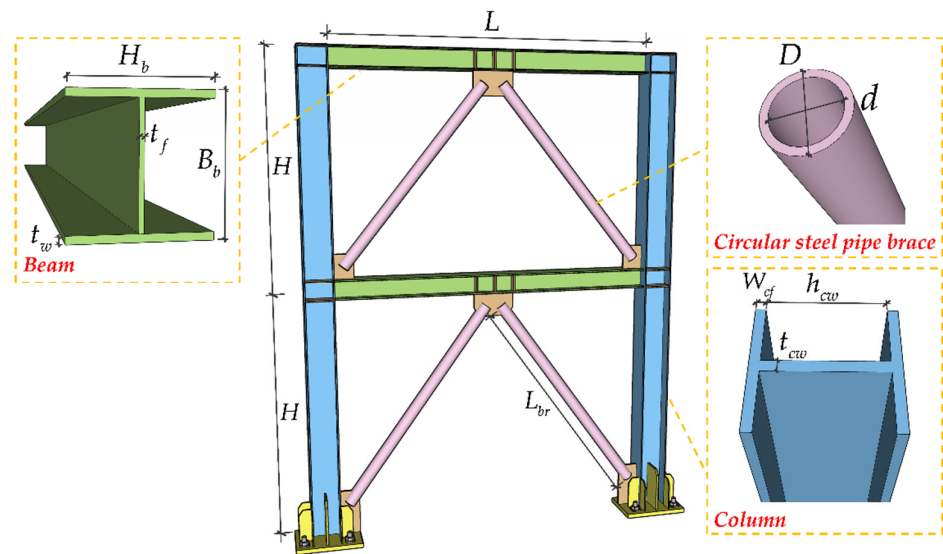


Figure 1. The components of a steel concentrically-braced frame.

2.1. Component Bearing Capacity

The beam obtains the maximum yield strength capacity, that is, the section will have a plastic hinge under bending stress. The beam’s plastic bending yield strength models could be calculated by the beam’s plastic section modulus (W_{pb}) and steel’s yield strength (f_y), defined as $M_{pb} = f_y W_{pb}$.

The braces can be assumed to be axially loaded, so their bending capacity could be ignored. So $M_{bry} = 0$. However, the influence of the braces on the beams must certainly be considered when evaluating a beam’s plastic yield strength. That is, the additional axial force on the beam at the brace’s yield state must be considered. The calculation for the plastic yield strength of a top floor beam is shown schematically in Figure 2a.

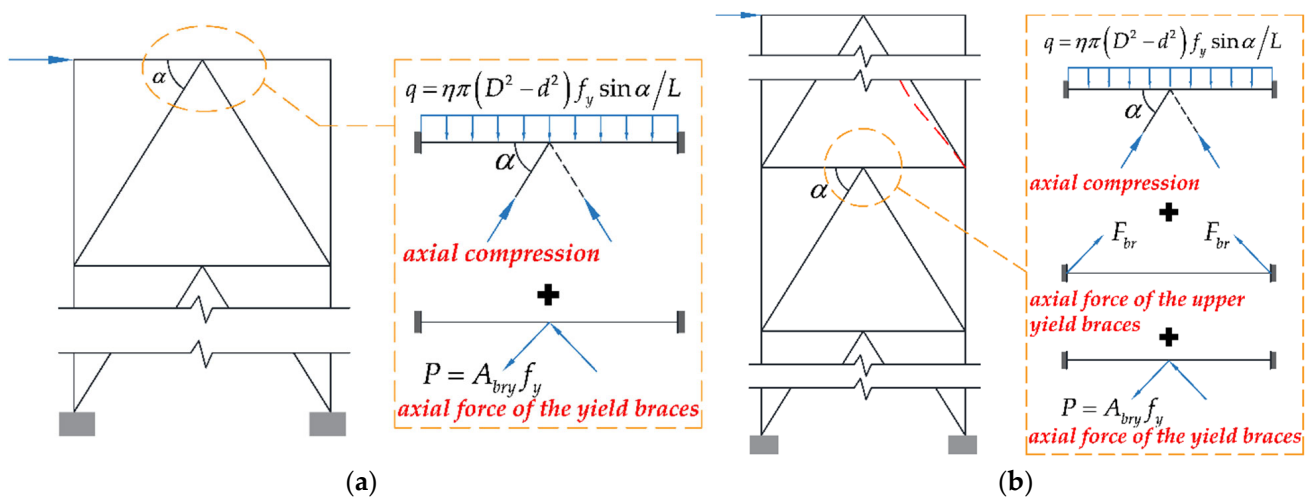


Figure 2. Calculation schemas for the plastic bending yield strength of the beam. (a) a top floor beam affected by two braces; (b) a typical floor beam affected by four braces.

The model of a top floor beam must correctly represent the beam’s bearing capacity, the bending of the horizontal force exerted by the braces, and the bending of the vertical uniform force transferred from the braces’ axial compression, as shown in Equation (1).

$$M_{pbc} = f_y W_{pb} - \frac{2(2 - 2\eta)W_{pb}P \cos \alpha}{A_b} - \frac{qL^2}{48} \tag{1}$$

In Equation (1), W_{pb} is the plastic section modulus of the beam; A_b is the beam's cross-sectional area; f_y is the steel's yield strength; L is the beam's length; P is the axial force applied by (circular steel tube) braces when they yield. $P = A_{bry}f_y = \pi(D^2 - d^2)f_y/4$. A_{bry} is the brace's cross-sectional area. q is the uniform load on the beam based on η , the axial compression ratio of braces. For circular steel tube braces, $q = \eta\pi(D^2 - d^2)f_y\sin\alpha/L$. α is the angle between the beam and the brace.

The structural typical floor beam plastic model is different from the top ones, as shown in Figure 2b, the two upper braces need to be considered. The horizontal axial force acting on the beam by upper and lower braces, simultaneously. The typical floor beam plastic model could be used to calculate with Equation (2).

$$M'_{pbc} = f_y W_{pb} - \frac{W_{pb}[(2 - 2\eta)P + (1 - 2\eta)F_{br}] \cos \alpha}{A_b} - \frac{qL^2}{48} \quad (2)$$

where F_{br} is the axial force applied by the upper braces at yielding.

Chinese GB50017-2017 [3] specifies that the yield moment of a column panel-zone should be calculated as

$$M_{cy} = \frac{4f_y h_{bw} h_{cw} t_{cw}}{3\sqrt{3}} \quad (3)$$

where h_{bw} is the height of the beam's web; h_{cw} is the height of the column's web; t_{cw} is the thickness of the column's web.

2.2. Parameter Ranges (Top Floor Calculation)

2.2.1. Parameter Ranges of d

Firstly, consider d , the inside diameter of the tubular braces. The relationship between the bearing capacity of the beam and that of a brace requires that the beam should be able to resist the axial force from a brace up to the brace's yield strength. The constraint that the brace yields before the beam can be expressed as $M_{bpc} > 2M_{bry}$. With the inequality transformation analysis, d is then constrained, as shown in Equation (4).

$$d > \sqrt{D^2 - \frac{48W_{pb}A_b}{24\pi(1 - \eta)W_{pb} \cos \alpha + \eta\pi A_b L \sin \alpha}} = \Delta_1 \quad (4)$$

In addition, Chinese standardized (GB 50011-2010) requires that λ (the slenderness ratio of the braces) should be between $65\sqrt{235/f_y}$ and $120\sqrt{235/f_y}$ to prevent premature failure of the braces. The brace's welded connection can be assumed to be rigid, and its effective length factor could be defined as 0.5 in standard GB 50011-2010. With the inequality $\lambda > 65\sqrt{235/f_y}$ and $\lambda < 120\sqrt{235/f_y}$, d must therefore satisfy the constraints of both Equation (5) and Equation (6).

$$d > \sqrt{\frac{(4H^2 + L^2)f_y}{3,384,000} - D^2} = \Delta_2 \quad (5)$$

$$d < \sqrt{\frac{(4H^2 + L^2)f_y}{992,875} - D^2} = \Delta_3 \quad (6)$$

where H is the height of the structural floor.

Standard GB 50011-2010 also requires that the ratio of brace width to thickness should be less than $9870/f_y$. So d has the constraint expressed in Equation (7).

$$d < D \left(1 - \frac{f_y}{4935}\right) = \Delta_4 \quad (7)$$

So, if the braces must be yielded before the beams, the inner diameter of the braces must satisfy Equation (8).

$$\max\{0, \Delta_1, \Delta_2\} < d < \min\{\Delta_3, \Delta_4, D\} \quad (8)$$

2.2.2. Parameter Ranges of D

Turning to the outer diameter D , having established Equation (8), then $D > d$, $D > \Delta_1$, $D > \Delta_2$, $\Delta_4 > 0$, $\Delta_4 > \Delta_1$, $\Delta_4 > \Delta_2$, $\Delta_3 > 0$, $\Delta_3 > \Delta_1$ and $\Delta_3 > \Delta_2$ must all be satisfied, concurrently. $\Delta_2 > 0$ and $\Delta_1 > 0$ must be established for a given D .

When $\Delta_3 > 0$, D should satisfy:

$$D < \sqrt{\frac{(4H^2 + L^2)f_y}{992,875}} = \Delta_5 \quad (9)$$

When $\Delta_3 > \Delta_1$, D should satisfy:

$$D < \sqrt{\frac{24W_{pb}A_b}{24\pi(1-\eta)W_{pb}\cos\alpha + \eta\pi A_b L \sin\alpha} + \frac{4H^2 + L^2}{1,985,750}f_y} = \Delta_6 \quad (10)$$

And if $\Delta_4 > \Delta_1$, then D should satisfy:

$$D < \sqrt{\frac{48W_{pb}A_b}{\left[1 - \left(1 - \frac{f_y}{4935}\right)^2\right] \left[24\pi(1-\eta)W_{pb}\cos\alpha + \eta\pi A_b L \sin\alpha\right]}} = \Delta_7 \quad (11)$$

As long as $\Delta_1 > 0$, then,

$$D > \sqrt{\frac{48A_b}{24\pi(1-\eta)W_{pb}\cos\alpha + \eta\pi A_b L \sin\alpha}} = \Delta_8 \quad (12)$$

When $\Delta_4 > \Delta_2$,

$$D > \sqrt{\frac{(4H^2 + L^2)f_y}{3,384,000 \left[1 + \left(1 - \frac{f_y}{4935}\right)\right]}} = \Delta_9 \quad (13)$$

And if $D > \Delta_2$, then Equation (14) should be satisfied.

$$D > \sqrt{\frac{(4H^2 + L^2)f_y}{6,768,000}} = \Delta_{10} \quad (14)$$

Thus, if the braces are to yield first,

$$\max\{0, \Delta_8, \Delta_9, \Delta_{10}\} < D < \min\{\Delta_5, \Delta_6, \Delta_7\} \quad (15)$$

2.2.3. Parameter Ranges of Column

$M_{cy} > M_{pbc}$ is a necessary condition to ensure that the beams yield before the columns. In other words, in the *strong column and weak beam* criterion, the column's elastic bending yield strength is stronger than the beam's plastic bending yield strength. The column's web area should therefore satisfy Equation (16), which is derived from an inequality analysis of the beam and column-bearing capacity models.

$$h_{cw}t_{cw} > \frac{3\sqrt{3}}{4f_y h_{bw}} f_y W_{pb} = \Delta_{11} \quad (16)$$

At the same time, practical considerations require that the width of the column's flange should be longer than that of the beam.

$$w_{cf} > w_{bf} = \Delta_{12} \quad (17)$$

2.3. Parameter Ranges (Typical Floor Calculation)

2.3.1. Parameter Ranges of d

On a typical floor, four braces act on a beam or column, so the inequalities need to be modified. If $M'_{bpc} > 2M_{bry}$, the inner diameter of the brace should satisfy:

$$d > \sqrt{D^2 - \frac{48A_b W_{pb} f_y - 48(1 - 2\eta) F_{br} W_{pb} \cos \alpha}{24\pi(1 - \eta) f_y W_{pb} \cos \alpha + \eta \pi f_y A_b L \sin \alpha}} = \Delta_{13} \quad (18)$$

Moreover, Equations (5)–(7), and (18) still apply, so

$$\max\{0, \Delta_{13}, \Delta_2\} < d < \min\{\Delta_3, \Delta_4, D\} \quad (19)$$

2.3.2. Parameter Ranges of D

Equation (19) then requires that $D > d$, $D > \Delta_{13}$, $D > \Delta_2$, $\Delta_4 > 0$, $\Delta_4 > \Delta_{13}$, $\Delta_4 > \Delta_2$, $\Delta_3 > 0$, $\Delta_3 > \Delta_{13}$, and $\Delta_3 > \Delta_2$. That $D > \Delta_{13}$, $D > 0$, $D > \Delta_2$, $\Delta_4 > 0$, $\Delta_4 > \Delta_2$, $\Delta_3 > 0$, and $\Delta_3 > \Delta_2$ has already been established. That $\Delta_3 > \Delta_{13}$, $\Delta_4 > \Delta_{13}$ and $\Delta_{13} > 0$ must be proved with the ranges of the D .

When $\Delta_3 > \Delta_{13}$, D should satisfy:

$$D < \sqrt{\frac{24A_b W_{pb} f_y - 24(1 - 2\eta) F_{br} W_{pb} \cos \alpha}{24\pi(1 - \eta) f_y W_{pb} \cos \alpha + \eta \pi f_y A_b L \sin \alpha} + \frac{4H^2 + L^2}{1985750} f_y} = \Delta_{14} \quad (20)$$

When $\Delta_4 > \Delta_{13}$, D should satisfy:

$$D < \sqrt{\frac{48A_b W_{pb} f_y - 48(1 - 2\eta) F_{br} W_{pb} \cos \alpha}{\left[1 - \left(1 - \frac{f_y}{4935}\right)^2\right] \left[24\pi(1 - \eta) f_y W_{pb} \cos \alpha + \eta \pi f_y A_b L \sin \alpha\right]}} = \Delta_{15} \quad (21)$$

And when $\Delta_3 > \Delta_{13}$,

$$D > \sqrt{\frac{48A_b W_{pb} f_y - 48(1 - 2\eta) F_{br} W_{pb} \cos \alpha}{24\pi(1 - \eta) f_y W_{pb} \cos \alpha + \eta \pi f_y A_b L \sin \alpha}} = \Delta_{16} \quad (22)$$

So Equations (9), (13), (14), (20)–(22) together require that the D of the braces on a typical floor should satisfy:

$$\max\{0, \Delta_{16}, \Delta_9, \Delta_{10}\} < D < \min\{\Delta_5, \Delta_{14}, \Delta_{15}\} \quad (23)$$

Meanwhile, according to the relationship between the beam's plastic bending yield strength and the column's elastic bending yield strength, the range of column parameters for a typical floor should be the same as for the top floor. And the web area and flange width for the columns can be calculated with Equations (16) and (17).

2.4. Structural Parameter Ranges Calculation Method of Other Sections

The proposed method can be applied to any steel frame that is concentrically braced, but the beam model needs to be changed by changing the brace area calculation method. Figure 3 defines the parameters of square steel tube braces. The inner length is now l_s and the external length is L_s . In addition, a brace's axial force and axial compression ratio

(Equations (1) and (2)) need to be changed with $P = A_{bry}f_y = (L_s^2 - l_s^2)f_y$, and $q = 4\eta(L_s^2 - l_s^2)f_y \sin\alpha / L$.

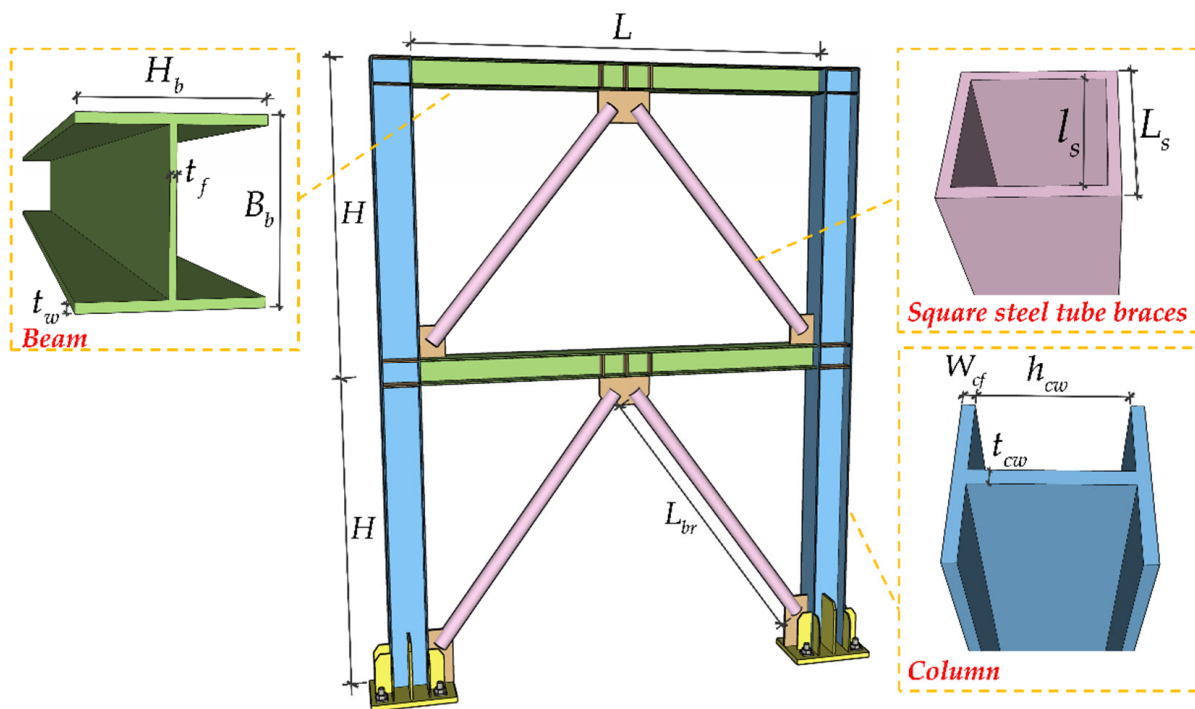


Figure 3. The parameters of a square steel tube brace.

2.4.1. Parameter Ranges of l_s (Top Floor)

Treating first the top floor, the range for a square steel tube brace’s inner length can be calculated using the inequality relating the beam’s plastic bending bearing strength with the influence of the brace’s axial force and bending strength, as shown in Equation (24).

$$\max\{0, \Delta_{s1}, \Delta_{s2}\} < l_s < \min\{\Delta_{s3}, \Delta_{s4}, L_s\} \tag{24}$$

Then, using the same inequality recurrence method as the circular steel tube braces, Δ_{s1} can be calculated using the inequality relating to the beam’s plastic bending yield strength and the brace bending yield strength, as shown in Equation (25). The Δ_{s2} , Δ_{s3} , and Δ_{s4} can be obtained from the limits on the brace’s slenderness ratio and width-thickness ratio, as shown in Equations (26)–(28).

$$l_s \geq \sqrt{D_s^2 - \frac{12W_{pb}A_b}{24(1 - \eta)W_{pb} \cos \alpha + \eta A_b L \sin \alpha}} = \Delta_{s1} \tag{25}$$

$$l_s \geq \sqrt{\frac{(12H^2 + 3L^2)f_y}{13,936,000} - D_s^2} = \Delta_{s2} \tag{26}$$

$$l_s \leq \sqrt{\frac{(12H^2 + 3L^2)f_y}{3,971,500} - D_s^2} = \Delta_{s3} \tag{27}$$

$$l_s \leq D_s \left(1 - \sqrt{\frac{f_y}{52,875}} \right) = \Delta_{s4} \tag{28}$$

2.4.2. Parameter Ranges of L_s (Top Floor)

At the top floor, the range for the brace's external length (L_s) can be obtained with the inequalities transformation analysis of $\Delta_{s3} > 0$, $\Delta_{s3} > \Delta_{s1}$, $\Delta_{s4} > \Delta_{s1}$, $\Delta_{s4} > \Delta_{s2}$ and $L_s > \Delta_{s2}$, as shown in Equation (29).

$$\max\{0, \Delta_{s7}, \Delta_{s10}\} < L_s < \min\{\Delta_{s6}, \Delta_{s8}, \Delta_{s9}\} \quad (29)$$

Equations (30)–(34) can then be calculated with the inequalities $\Delta_{s3} > 0$, $\Delta_{s3} > \Delta_{s1}$, $\Delta_{s4} > \Delta_{s1}$, $\Delta_{s4} > \Delta_{s2}$ and $L_s > \Delta_{s2}$.

$$L_s \leq \sqrt{\frac{(12H^2 + 3L^2)f_y}{3,971,500}} = \Delta_{s6} \quad (30)$$

$$L_s \geq \sqrt{\frac{(12H^2 + 3L^2)f_y}{27,072,000}} = \Delta_{s7} \quad (31)$$

$$L_s \leq \sqrt{\frac{6A_b W_{pb}}{24(1-\eta)W_{pb} \cos \alpha + \eta A_b L \sin \alpha} + \frac{(12H^2 + 3L^2)f_y}{7,943,000}} = \Delta_{s8} \quad (32)$$

$$L_s \leq \sqrt{\frac{12A_b W_{pb}}{\left[1 - (1 - \sqrt{f_y/52,875})^2\right] \left[24(1-\eta)W_{pb} \cos \alpha + \eta A_b L \sin \alpha\right]}} = \Delta_{s9} \quad (33)$$

$$L_s \geq \sqrt{\frac{(12H^2 + 3L^2)f_y}{13,536,000 \left[1 + (1 - \sqrt{f_y/52,875})^2\right]}} = \Delta_{s10} \quad (34)$$

2.4.3. Parameter Ranges of l_s and L_s (Typical Floor)

The other floors are again somewhat different, but the inner external length ranges for square steel tube braces can be calculated with the same method used with the circular ones. The inner length range is given by Equations (35) and (36), and the external length range is defined by Equations (37)–(39).

$$\max\{0, \Delta_{s11}, \Delta_{s2}\} < l_s < \min\{\Delta_{s3}, \Delta_{s4}, L_s\} \quad (35)$$

$$l_s \geq \sqrt{L_s^2 - \frac{12W_{pb} [A_b f_y - (1 - 2\eta)F_{br} \cos \alpha]}{24(1-\eta)W_{pb} f_y \cos \alpha + \eta f_y A_b L \sin \alpha}} = \Delta_{s11} \quad (36)$$

$$\max\{0, \Delta_{s7}, \Delta_{s10}\} < L_s < \min\{\Delta_{s6}, \Delta_{s12}, \Delta_{s13}\} \quad (37)$$

$$L_s \leq \sqrt{\frac{6W_{pb} [A_b f_y - (1 - 2\eta)F_{br} \cos \alpha]}{24(1-\eta)W_{pb} f_y \cos \alpha + \eta A_b f_y L \sin \alpha} + \frac{(12H^2 + 3L^2)f_y}{7,943,000}} = \Delta_{s12} \quad (38)$$

$$L_s \leq \sqrt{\frac{12W_{pb} [A_b f_y - (1 - 2\eta)F_{br} \cos \alpha]}{\left[1 - (1 - \sqrt{f_y/52,875})^2\right] \left[24(1-\eta)W_{pb} f_y \cos \alpha + \eta A_b f_y L \sin \alpha\right]}} = \Delta_{s13} \quad (39)$$

Before the braces yield, the bearing capacity of the beams and columns should not be influenced by the axial force from the braces. The ranges for the column are still those of Equations (16) and (17), and that ensures the structure meets the yield mechanism control criteria.

3. Experimental Verification of the Method

3.1. Top Floor

Seven published test results of small, braced structures were used to demonstrate the proposed method. As [10,21–23], the story height and span of specimen SCBF-1 were

3000 mm × 6000 mm, of TCBF-B-1 were 2743 mm × 6096 mm, of SP1 were 3297 mm × 6286 mm, and those of Chevron 2, 3, 4, and 6 were all 3183 mm × 6172 mm. Table 2 gives the beam, column, and brace dimensions. The axial compression ratio of the specimens' braces was designed as 0. The column bases and beam-column joints were set as rigid connections, and constraints were set out-of-plane of structures to avoid lateral instability, as shown in Figure 4. All the specimens were laterally pushed with a low cycle reciprocating hysteretic load. Moreover, the load position of specimens SCBF-1, TCBF-B-1, and SP1 were set at the external of unilateral beam-column joints, and Chevron 2, 3, 4, and 6 were set at both side column caps.

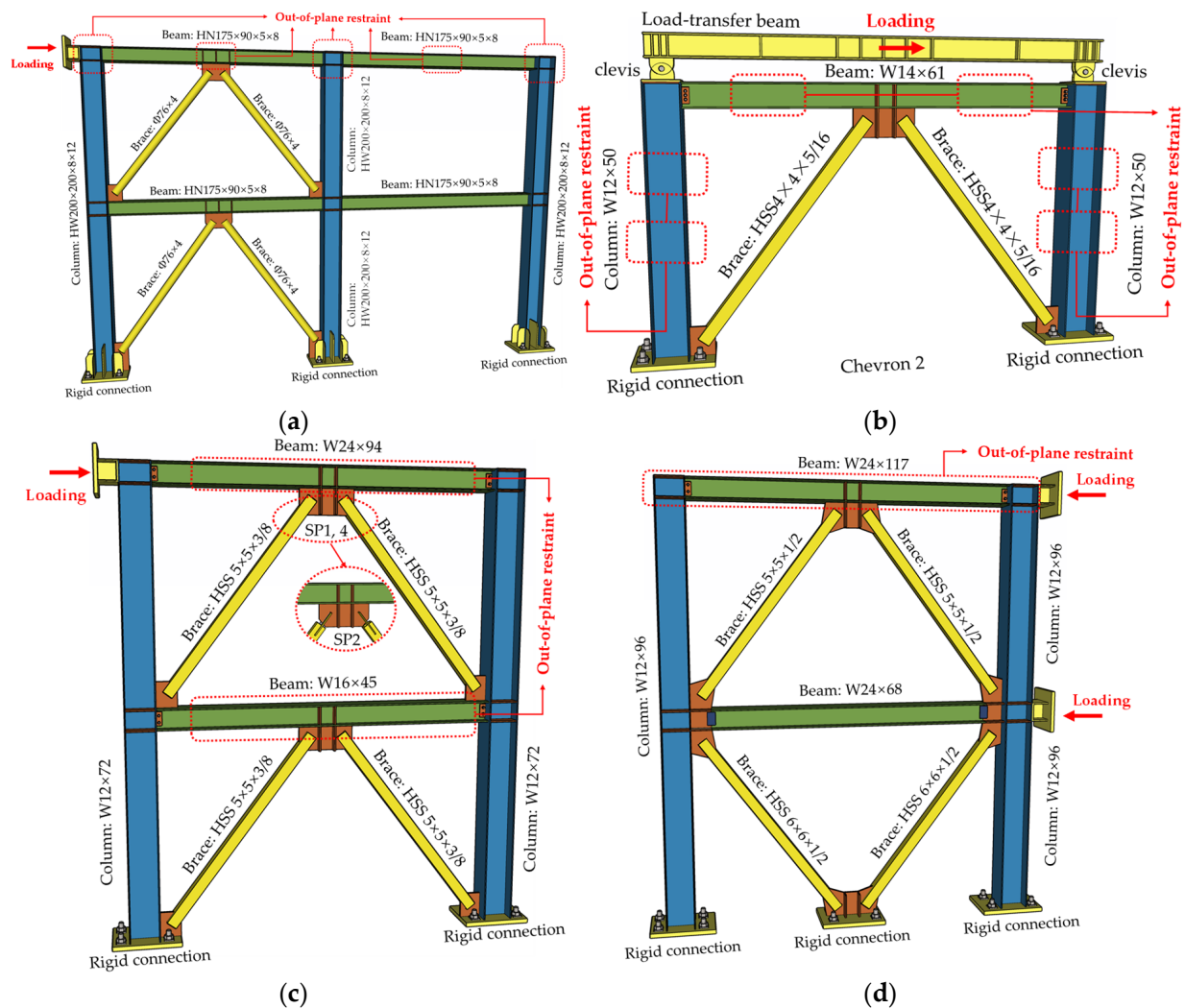


Figure 4. Published test specimens and set up. (a) SCBF [21]; (b) Chevron [23]; (c) SP [10]; (d) TCBF-B-2 [22].

Substituting those parameters into Equations (1)–(17) and (24)–(34) for iterative calculation yielded the ranges for the column web area ($h_{cw}t_{cw}$), the column flange width (w_{cf}), the brace external diameter (D), the brace inner diameter (d), the brace external length (D_s), and the brace inner length (d_s) shown in Table 2. If a component size of a test specimen was not within the parameter range obtained by the proposed method, it was set at the range's boundary value. As the table shows, the column and brace sizes of specimens SCBF-1, TCBF-B-1, SP1, and Chevron 2, 3, 4, and 6 were within the ranges. Indeed, the test results show bracing yielded first under lateral loading, consistent with the yield mechanism control criterion.

3.2. Typical Floor

Four published test results of small two-story braced structures were used to demonstrate the proposed method with a typical floor. As [10,21,23], the story height and span of specimen SCBF-2 were 3000×6000 mm. For SP2 and SP4, they were 3297×6286 mm, and for Chevron R, they were $4570 \times 10,700$ mm. The beams, columns, and bracing were as described in Table 3, and the axial compression ratio was again 0. The top beam and column were the same size as the bottom ones in all four cases. All specimens were designed with rigid connections of column base and beam-to-column joints. As the top structure, the out-of-plane constraints were set to avoid lateral instability. Furthermore, the low-cycle reciprocating hysteretic load was used to test the structure's laterally bearing capacity. The load position of specimen SCBF-2, SP2, and SP4 was set at the external of the second-floor unilateral beam-column joints. Chevron R was at both sides of the second-floor column caps.

Substituting the story height, the span, and the components' sizes into Equations (1)–(3), (16)–(23), and (35)–(39) for the iterative calculation, yielded the ranges for the typical column web area ($h_{cw}t_{cw}$), the typical column flange width (w_{cf}), the typical brace external diameter (D), the typical brace inner diameter (d), the typical brace external length (D_s), and the typical brace inner length (d_s) shown in Table 3. The component sizes for specimens SCBF-2, SP2, and SP4 were within their ranges. The bracing yields first, followed by the beams and then the columns. However, that sequence changes with component sizes outside the parameter range constraints. Chevron R's brace lengths were larger than the prescribed range, which gave the bracing bearing capacity beyond that of the beams. So with Chevron R, the beams yielded first, which was consistent with the predictions calculated using the proposed method. The proposed method thus seems effective for controlling the yield sequence.

Table 2. Experimental verification results (top floor).

Specimen ID	Beam (mm or in)	Column Constraint			Brace Constraint (mm)			Test Result	Proposed Method
		Column (mm or in)	Web Constraint (mm ²)	Flange Constraint (mm)	Brace (mm or in)	External Diameters Constraint	Inner Diameters Constraint		
SCBF-1 [21]	HN175 × 90 × 5 × 8	HW200 × 200 × 8 × 12	$h_{cw}t_{cw} > 1095$	$w_{cf} > 90$	$\Phi 76 \times 4$	$61 < D < 122$	$66 < d < 93$	Brace Yielding	Brace Yielding
TCBF-B-2 [22]	W24 × 117 ¹	W12 × 96 ¹	$h_{cw}t_{cw} > 10708$	$w_{cf} > 325$	HSS5 × 5 × $\frac{1}{2}$ ¹	$61 < L_s < 129$	$87 < l_s < 91$	Brace Yielding	Brace Yielding
SP1 [10]	W24 × 94	W12 × 72	$h_{cw}t_{cw} > 8164$	$w_{cf} > 230$	HSS5 × 5 × 3/8	$63 < L_s < 131$	$87 < l_s < 95$	Brace Yielding	Brace Yielding
Chevron 2 [23]	W14 × 61	W12 × 50	$h_{cw}t_{cw} > 6017$	$w_{cf} > 254$	HSS4 × 4 × 5/16	$61 < L_s < 127$	$61 < l_s < 93$	Brace Yielding	Brace Yielding
Chevron 3 [23]	W14 × 38	W12 × 50	$h_{cw}t_{cw} > 3452$	$w_{cf} > 172$	HSS4 × 4 × 5/16	$58 < L_s < 116$	$72 < l_s < 94$	Brace Yielding	Brace Yielding
Chevron 4 [23]	W14 × 26	W12 × 50	$h_{cw}t_{cw} > 2209$	$w_{cf} > 128$	HSS4 × 4 × 5/16	$58 < L_s < 112$	$82 < l_s < 94$	Brace Yielding	Brace Yielding
Chevron 6 [23]	W21 × 44	W12 × 50	$h_{cw}t_{cw} > 3377$	$w_{cf} > 165$	HSS4 × 4 × 5/16	$61 < L_s < 122$	$66 < l_s < 93$	Brace Yielding	Brace Yielding

¹ The unit of W and HSS steel is inches.**Table 3.** Experimental verification results (typical floor).

Specimen ID	Upper Brace (mm or in)	Beam (mm or in)	Column Constraint			Brace Constraint (mm)			Test Result	Proposed Method
			Column (mm or in)	Web Constraint (mm ²)	Flange Constraint (mm)	Brace (mm or in)	External Diameters Constraint	Inner Diameters Constraint		
SCBF-2 [21]	$\Phi 76 \times 4$	HN175 × 90 × 5 × 8	HW200 × 200 × 8 × 12	$h_{cw}t_{cw} > 1095$	$w_{cf} > 90$	$\Phi 76 \times 4$	$53 < D < 98$	$65 < d < 72$	Brace Yielding	Brace Yielding
SP2 [10]	HSS7 × 7 × 1/4	W16 × 45	W12 × 72	$h_{cw}t_{cw} > 4009$	$w_{cf} > 179$	HSS5 × 5 × 3/8	$63 < L_s < 121$	$102 < l_s < 103$	Brace Yielding	Brace Yielding
SP4 [10]	HSS5 × 5 × 3/8	W16 × 45	W12 × 72	$h_{cw}t_{cw} > 4009$	$w_{cf} > 179$	HSS5 × 5 × 3/8	$63 < L_s < 121$	$102 < l_s < 103$	Brace Yielding	Brace Yielding
Chevron R [23]	HSS8 × 8 × 1/4	W12 × 40	W12 × 53	$h_{cw}t_{cw} > 3875$	$w_{cf} > 203$	HSS8 × 8 × 3/8	$91 < L_s < 124$	$112 < l_s < 113$	Beam Yielding	Beam Yielding

4. Verification by Finite Element Modeling

4.1. Material Properties

The steel of the columns, beams, braces, stiffeners, and connecting plates model was Q345 grade with an elasticity modulus of 206,000 Mpa, a Poisson's ratio of 0.3, a yield strength of 345 MPa, and a tensile strength of 580 MPa. Figure 5 shows the trilinear constitutive model used for the Q345 steel [24].

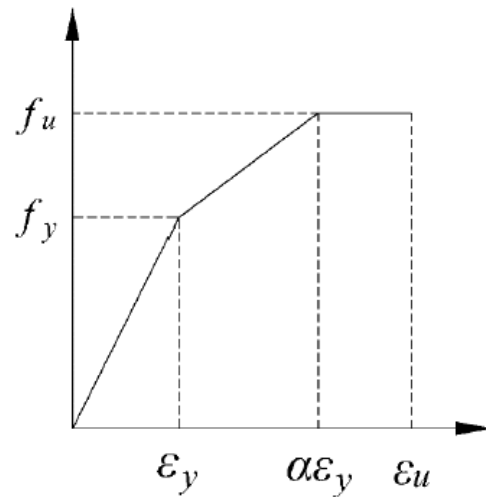


Figure 5. Constitutive model of the steel plate.

4.2. Modeling

Hexagonal reduced integration elements with eight nodes (C3D8R) were used in the FE models. The global and local mesh sizes of the columns, braces, and beams were 50 mm and 15 mm, respectively, while the connecting plates meshed at 15 mm (Figure 6).

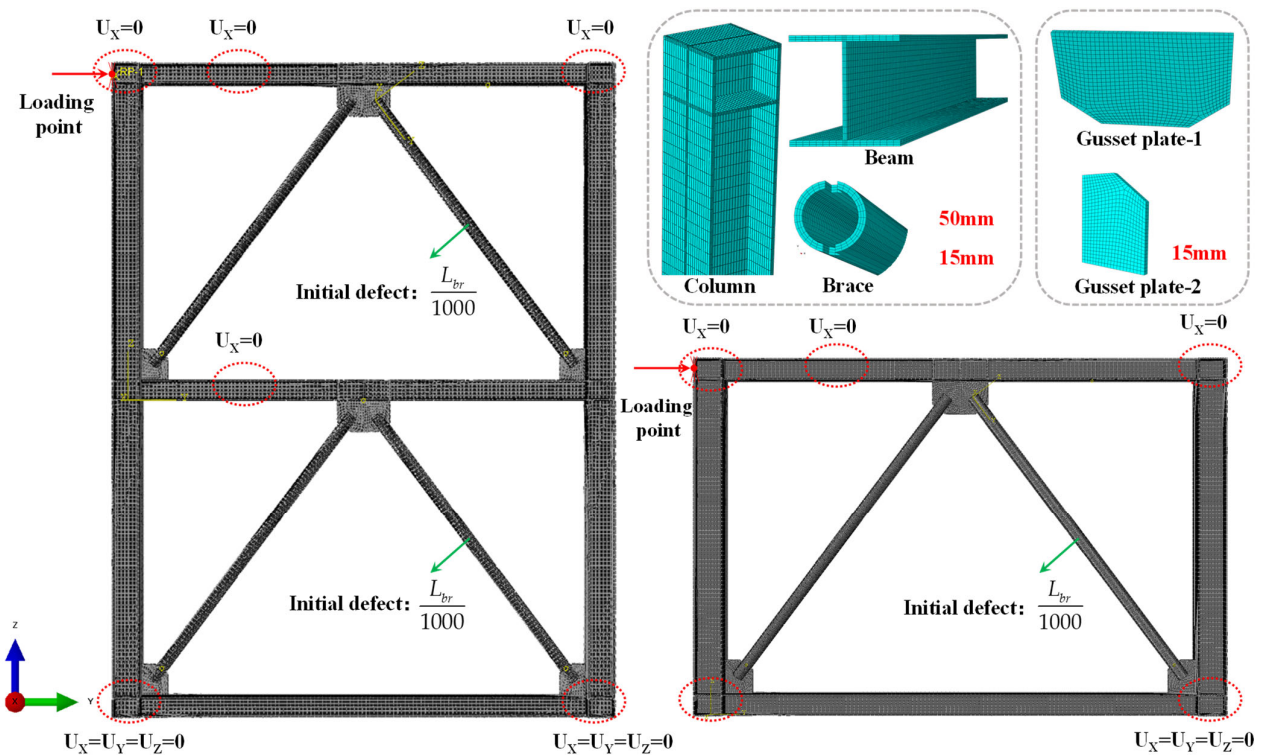


Figure 6. Details of the FE model of a concentrically-braced steel frame.

In the proposed method, the weld fracture failure of the structure is not considered. Tie constraints connected the components, giving the joints rotational stiffness close to rigid due to the strengthening effect of the gusset plates. The welds between columns and beams were also represented with tie constraints.

To avoid local deformation under concentrated forces, the loading points were coupled to the boundary surfaces of the column through coupling constraints. As in [21], the bottom surfaces of the column were constrained in all three directions. To prevent out-of-plane deformations, the flanges of the beam and the top surfaces of the column restrictions were restricted to the Y-Z plane.

The loading was in two steps. An out-of-plane deformation of one one-thousandth of the brace's length was first applied in the brace's span as an initial defect to stimulate possible instability. Displacement-controlled loading was then applied to the coupling point at the top of the column. It ended at 1/50 of the story drift angle.

4.3. Validation of Finite Element Modeling

A three-story concentrically-braced steel frame test result has been published [25], and it was compared with the FE results to verify the accuracy of the numerical modeling process. The geometrical configurations of the specimen's component was designed as HW 150 × 150 × 7 × 10 mm (columns), HM 200 × 150 × 6 × 9 mm (top floor beam), HM 150 × 100 × 6 × 9 mm (first and second-floor beam), and HN 100 × 50 × 5 × 7 mm (braces). The steel of the components was Q235B, and the nominal yield strength was 235 MPa.

The deformation pattern of the specimen observed in FE is presented in Figure 7a, and the load-displacement curves of the specimen are shown in Figure 7b. As can be seen, the out-of-plane deformation of the first and second-floor braces was observed at the peak load, but the out-of-plane deformation of the three-floor braces was observed at 35 mm loading displacement. Its deformation patterns are similar to experiments. The curves obtained from the FE simulation agree well with those observed. This suggests that numerical modeling can be considered accurate enough for subsequent parametric analysis.

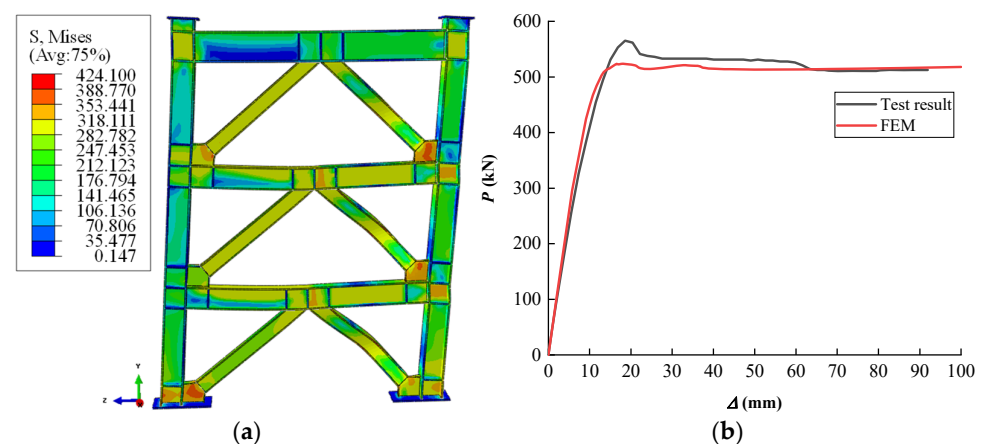


Figure 7. Validation result of finite element modeling. (a) deformation of a three-story concentrically-braced steel frame; (b) load-displacement curves from experiment and the FE analysis.

4.4. Finite Element Modeling Parameters

With the limited experimental data, it is difficult to fully verify the accuracy of the proposed method. Finite element modeling offers an alternative approach. To study the influence of the component parameter ranges on the yield mechanism, 48 concentrically-braced steel frames with different parameters were modeled. All of the frames modeled were 6000 mm tall and 4000 mm square. The beams were designed to be 250 mm high (H_b) × 250 mm width (B_b) with a web thickness t_{bw} of 9 mm and a flange thickness t_{bf} of 14 mm. The other component parameters were obtained by the proposed method.

On the top floor, FE model Equations (9)–(14) were used. With an axial compression ratio in the braces of 0, the constraint boundaries are $\Delta_5 = 186$ mm, $\Delta_6 = 148$ mm, $\Delta_7 = 237.5$ mm, $\Delta_8 = 70$ mm, $\Delta_9 = 73.9$ mm and $\Delta_{10} = 71.4$ mm. That gives 74 mm $< D < 148$ mm. The lower limit is the ceiling maximum of 0, Δ_8 , Δ_9 , and Δ_{10} , and the upper limit is the rounding minimum of Δ_5 , Δ_6 , and Δ_7 . The external diameter was, therefore, defined as 140 mm in calculating the inner diameter of the top floor braces.

Substituting into the Equations (4)–(7), the constraint boundaries are $\Delta_1 = 100.2$ mm, $\Delta_3 = 123.07$ mm, and $\Delta_4 = 130.2$ mm. With $\Delta_2 < 0$, the brace slenderness requirement is met. The range for the inner diameter of the top floor braces is then 101 mm $< d < 123$ mm. The lower limit is the ceiling maximum of 0, Δ_1 , and Δ_2 , and the upper limit is the rounding minimum of D , Δ_3 , and Δ_4 . The inner diameter was, therefore, defined as 110 mm.

Substituting into Equations (16) and (17) yields the constraint boundaries $\Delta_{11} = 5771.5$ mm² and $\Delta_{12} = 250$ mm could be calculated. The ranges for the column are $h_{cw}t_{cw} > 5771.5$ mm² and $w_{cf} > 250$ mm. So, in the FE models, the columns were defined as $350 \times 350 \times 19 \times 19$. To prevent out-of-plane deformation and bending failure, the gusset plate should be designed to have a larger bearing capacity than other components. As [23], the geometric configurations of a gusset plate are designed with the proposed method, but the thickness is designed to be two times the brace's thickness.

The component parameters in the top floor FE models were changed to verify the accuracy of the yield mechanism control method. The parameters used are shown in Table 4. Case 1 is the basic model with component parameters within the ranges calculated by the proposed method. In case 2, the column panel-zone area was designed smaller to study the influence of changing column parameters on the yield mechanism. Smaller inner diameter braces were designed in case 3, and larger inner diameters were designed in case 4 to study the influence of the inner diameter on the yield control. Cases 5 and 6 tested the influence of the external thickness with larger external diameters in case 5 and smaller ones in case 6.

Table 4. Finite element verification results (top floor, $\eta = 0$).

Case	Column Section (mm)	Brace Section (mm)		Proposed Method	FEM Result
		External Diameters	Thickness		
1	HW 350 × 350 × 19 × 19	140	15	Brace Yielding	Brace Yielding
2	HW 344 × 348 × 10 × 16	140	15	Column Yielding before the beam	Column Yielding before the beam
3	HW 350 × 350 × 19 × 19	140	20	Beam Yielding	Beam Yielding
4	HW 350 × 350 × 19 × 19	140	8	Brace Yielding	Brace Yielding
5	HW 350 × 350 × 19 × 19	150	20	Beam Yielding	Beam Yielding
6	HW 350 × 350 × 19 × 19	74	15	Brace Yielding	Brace Yielding

In structural typical floor FE models, all the beam was designed as HW 250 × 250 × 9 × 14 mm, and the upper brace was designed with the influence of the brace axial compression ratio. As the axial compression ratio is 0, the braces were designed as $\Phi 140 \times 13$ mm (external diameter $D \times$ thickness t_{bry}). Inserting the parameters of the beam and the upper brace to the Equations (2), (3), (5)–(7), (9), (12)–(14), (16)–(18), (20)–(22), the ranges of the typical floor brace and the typical floor column could be calculated as follows.

- For brace axial compression ratio is 0, the ranges of braces' external diameters were calculated as 74 mm $< D < 144$ mm.
- Inserting the parameters of the beam and the external diameter, the ranges of the structural typical floor brace inner diameters were calculated as 115 mm $< d < 123$ mm.
- The ranges of column should be satisfied with $h_{cw}t_{cw} > 5771.5$ mm², $w_{cf} > 250$ mm.

The parameters of different structural typical floor components are shown in Table 5. Cases 7 is the basic models, which are obtained by the proposed method. Case 8 was designed with a smaller column panel-zone area. Case 9 was designed with smaller brace inner diameters. Case 10 was designed with larger brace inner diameters. Case 11 was

designed with larger brace external diameters. Case 12 was designed with smaller brace external diameters.

Table 5. Finite element verification results (typical floor, $\eta = 0$).

Case	Column Section (mm)	Brace Section (mm)		Proposed Method	FEM Result
		External Diameters	Thickness		
7	HW 350 × 350 × 19 × 19	140	12	Brace Yielding	Brace Yielding
8	HW 344 × 348 × 10 × 16	140	12	Column Yielding before the beam	Column Yielding before the beam
9	HW 350 × 350 × 19 × 19	140	14	Beam Yielding	Beam Yielding
10	HW 350 × 350 × 19 × 19	140	8	Brace Yielding	Brace Yielding
11	HW 350 × 350 × 19 × 19	144	14	Beam Yielding	Beam Yielding
12	HW 350 × 350 × 19 × 19	74	12	Brace Yielding	Brace Yielding

4.5. Top Floor Results

The finite element simulation results for the top floor, assuming different component parameters and axial compression ratios, are shown in Figure 8. They are consistent with the results of the theoretical calculations in terms of the yielding sequence, demonstrating the effectiveness of the proposed method. These top floor results with a 0 axial compression ratio also illustrate the relationship between the parameter range constraints and structural performance.

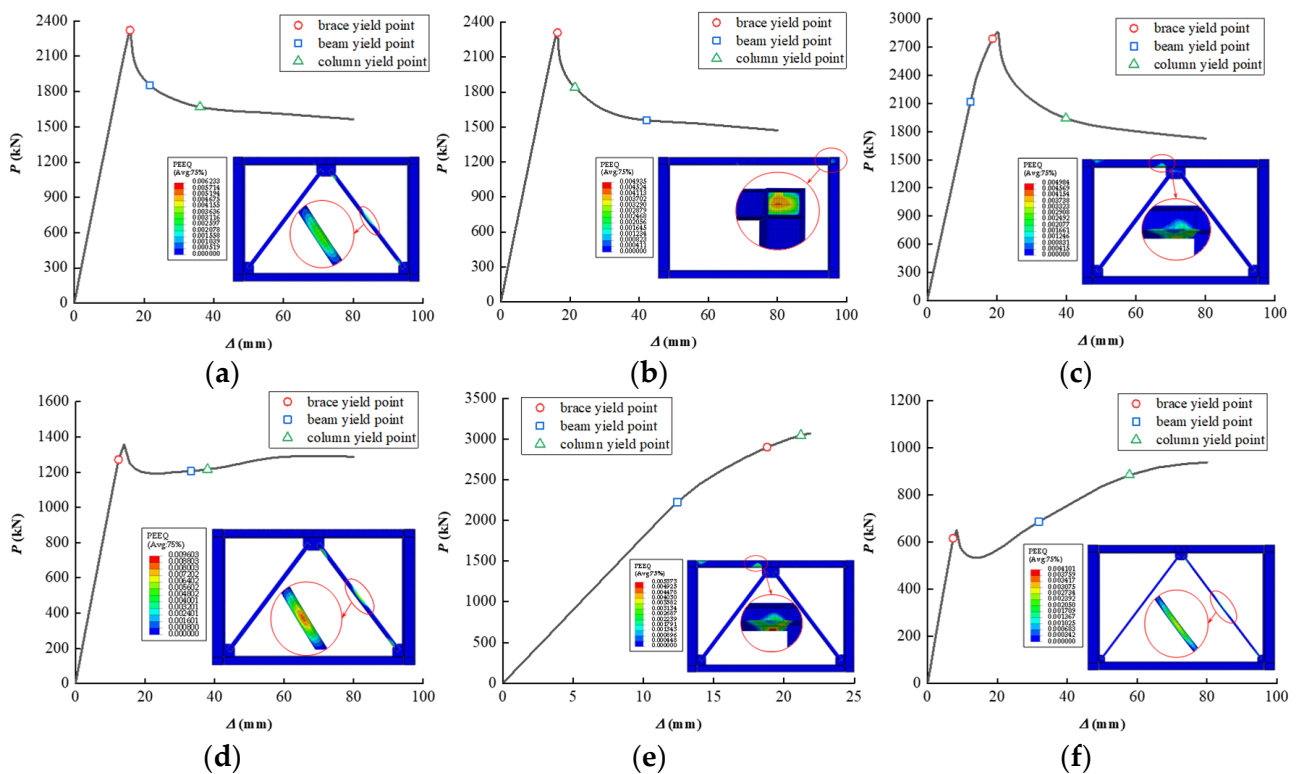


Figure 8. The predicted PEEQ (equivalent plastic strain) distributions of top floor concentrically-braced steel frames with different parameters ($\eta = 0$). (a) case 1, the basic model obtained by the proposed method; (b) case 2, with decreased section area of the column web; (c) case 3, with thicker braces; (d) case 4, with the thinner braces; (e) case 5, increasing external diameter of the braces; (f) case 6, decreasing the external diameter of the braces.

Comparing case 1 with case 2 (Table 4), the structure's bearing capacity was maintained at 2320 kN without obvious change despite using smaller columns. The braces yield first and simultaneously. However, the components' yield sequence with the weaker column in case 2 changes from the brace → beam → column to brace → column → beam.

Comparing the simulation results of cases 1 and 3, smaller-diameter, thicker braces increase the peak bearing capacity from 2320 kN to 2789 kN. The beam will be the first component to yield before the structure reaches its peak displacement, and its stiffness will be significantly decreased.

The finite element results of case 1 and case 4 show that increasing the inner diameter of the brace without changing the external diameter (thinner braces) reduces the bearing capacity, as to be expected. The peak lateral bearing capacity of case 4 was 1270 kN. The beam and the column yield at similar displacements. The yielding sequence is brace → beam → column.

Comparing the simulation results of cases 3 and 4, the larger external diameter of the brace in case 4 gives a greater lateral force bearing capacity of 3000 kN, though the structure is less ductile. Before loading to 22 mm, the structural components yield in the sequence brace → column → beam. However, case 3, with a brace with a smaller inner diameter, showed better ductility. The column yielded at 40 mm of displacement. Braces with a larger external diameter effectively improve the lateral stiffness of such concentrically-braced steel frames.

Turning to case 5, the brace with a smaller external diameter yields prematurely, and the structure's bearing capacity is significantly weakened. The maximum load was only 615 kN, 26% of that in case 1. Figure 8 shows how, after the brace yields, the lateral load is resisted by the frame, and the displacement increases only slowly until the beam and then the column yield. It is a brace → beam → column sequence. The braces don't provide sufficient energy dissipation and lateral resistance if they are too small.

Using the parameters in Table A1 in Appendix A, the different axial compression ratios simulated in Figures 8 and A1–A3 show that the components' yield sequence and displacement will not be changed with $\eta \leq 0.3$. The structure's bearing capacity, however, will decrease with the larger axial compression ratios. At the same time, due to the change in the ratio between the column's bearing capacity and the brace's bearing capacity, specimens with smaller braces are less affected by the axial compression ratios than larger ones. It will lead to the compression brace yield at a smaller displacement, and the energy dissipation capacity of braces cannot be fully used. Thus, within the range calculated by the proposed method, the larger brace's parameters should be selected to avoid the premature buckling of a brace.

4.6. Typical Floor Results

The finite element simulation results of a typical floor with four axial compression ratios and various component parameters are shown in Figure 9. As Table 5 shows, the theoretically calculated yield sequences agree with the predictions from the finite element modeling. Cases 7–12 were analyzed to illustrate the influence of different structural component parameter changes on the structural performance and the yield sequence. Consistent with the top story results, the yield sequence is brace → column → beam with the smaller columns. That is the sequence even with larger first-floor braces. With smaller braces, however, the yield sequence is brace → beam → column. Smaller-external diameter braces will fail under comparatively small loading and displacement, though thicker braces deliver greater bearing capacity at small external diameters.

Comparing case 1 with cases 7 and 8, smaller first-floor columns do not reduce the peak bearing capacity with the same bracing. However, the weaker columns force the bracing to resist more of the lateral load, and the brace's yield displacement decreases from 30 mm to 16 mm.

As the simulations of cases 7, 10, and 11 show, the structure's lateral bearing capacity was not improved with the different bracing. In cases 10 and 11, the structure's weakest components are the top-floor braces, beams, and columns. They directly influence the structure's performance. In addition, the beam yields first on the first floor, and its bracing greatly influences the beam's yield displacement. Braces with a larger external diameter have a smaller beam yield displacement. Thus, the stiffness difference

between the floor and its bracing should not be too large in such concentrically-braced steel frames. That will avoid the beams yielding prematurely and improve the structure's overall energy dissipation.

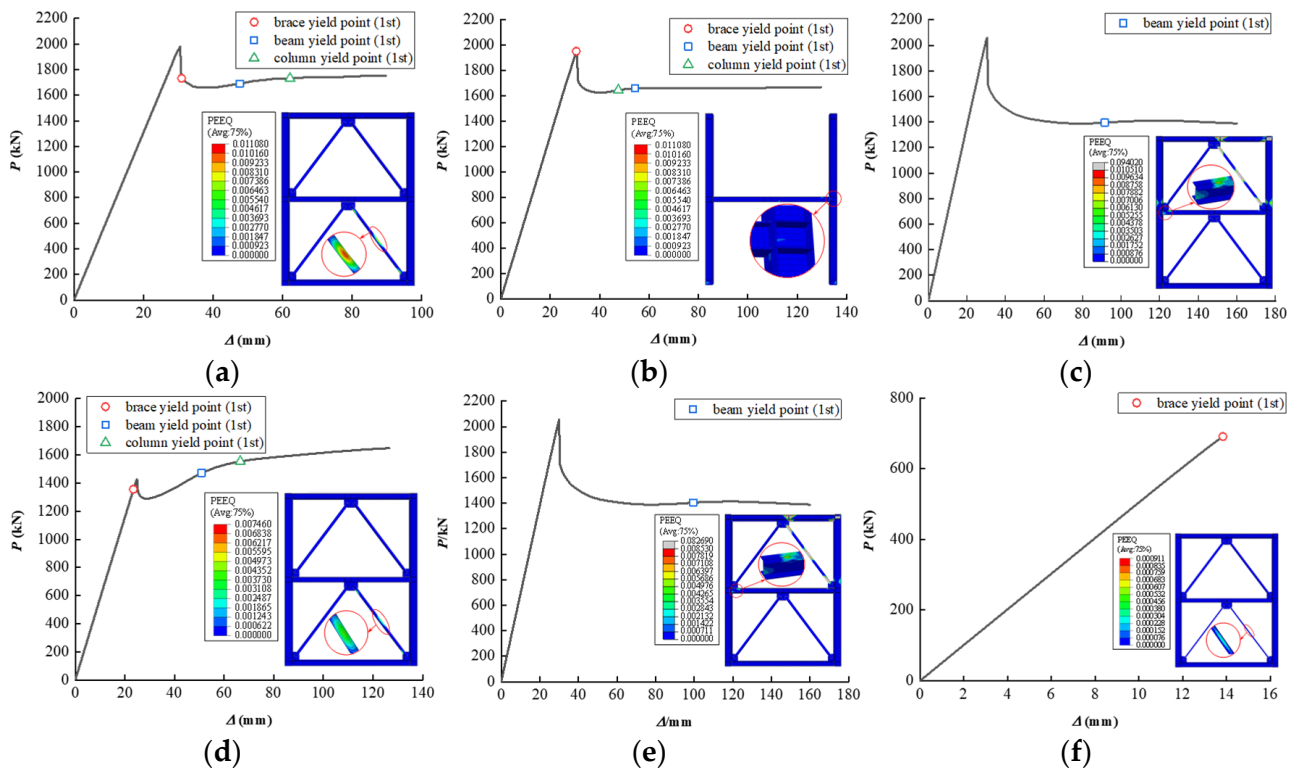


Figure 9. The predicted PEEQ distributions of concentrically-braced steel frames with different parameters (typical floor and $\eta = 0$). (a) case 7, the basic model obtained by the proposed method; (b) case 8, with a smaller-section column web; (c) case 9, with increased brace thickness; (d) case 10, with decreased brace thickness relative to the basic model; (e) case 11, with braces with larger external diameter; (f) case 12, with braces with smaller external diameter.

Comparing the simulation results of cases 7, 9, and 12 shows that the component yielding first will not be changed by reducing the brace's external diameter or increasing its inner diameter. However, the first-floor brace is the weakest component in cases 9 and 12. It yields first, which is different from case 7. The structure's peak bearing capacity will be greatly reduced from 1730 kN to 1355 kN and 690 kN. In addition, the models with smaller brace thicknesses predict weaker peak bearing capacity than in the cases with smaller external brace diameters. Thus, the external diameter of the braces should not be too small to avoid premature failure caused by excessive brace deformation.

Using the parameters in Table A2, the different axial compression ratios simulated in Figures 9 and A4–A6 show that the beam's bending bearing capacity will be weakened with the larger axial compression ratios under the lateral loading. The beam will induce local buckling in the brace at axial compression ratios greater than 0.3 under small lateral loads. That can be avoided by specifying stiffer beams in practical engineering. The beam's local strength should therefore be considered in yielding control with large axial compression ratios in the braces. In practice, however, there are few designs with an axial compression ratio greater than 0.3, so this study's proposed method should have excellent applicability in controlling the yield sequence.

5. Conclusions

In this paper, a technique for controlling the yielding of concentrically-braced steel frames has been proposed and demonstrated with the *strong column-weak beam* and *strong*

column and beam-weak brace criteria. It allows designing for an expected yield sequence despite a range of component parameters.

The following conclusions can be drawn from this study's observations.

- (1) The proposed method allows specifying the external diameter of the braces (D), their inner diameter (d), the web area of the columns ($h_{cw}t_{cw}$), and their flange thickness (w_{cf}) based on given beam parameters. That should be useful in performance-based design.
- (2) Published experimental results and finite element modeling has demonstrated that the sequence of component yielding will follow the method's predictions. The beam will yield first if the external or inner diameters of the braces are outside the ranges the method recommends. With a column web area smaller than the recommended minimum, the columns will yield first.
- (3) The axial compression in the braces significantly affects the yielding mechanism. The upper beam flange will be in a weak position under larger axial compression ($\eta > 0.3$). The beam ends and beam-brace connections should be stiffened to prevent local buckling.
- (4) The influence of stochastic variability in the parameters should be considered. Small changes in the parameters can change the structural yield sequence.
- (5) The proposed method helps to limit the initial feasible region in structure optimization. That will help to reduce convergence difficulties caused by the excessive size of the initial feasible region.

Author Contributions: Conceptualization, B.L. and Z.W.; methodology, B.L. and Z.W.; software, B.L. and Z.Z.; validation, B.L., Z.W., J.P. and P.W.; formal analysis, B.L. and Y.F.; investigation, B.L., Y.F. and Z.Z.; resources, B.L., Z.W. and J.P.; data curation, B.L. and Z.Z.; writing—original draft preparation, B.L. and Y.F.; writing—review and editing, Z.W., J.P. and P.W.; visualization, Y.F. and Z.Z.; supervision, Z.W., J.P. and P.W.; project administration, Z.W. and J.P.; funding acquisition, Z.W., J.P. and P.W. All authors have read and agreed to the published version of the manuscript.

Funding: This study was supported by China's National Natural Science Foundation (grants No. 51978279, 52278181), by the Guangdong Basic and Applied Basic Research Foundation (as project 2020A1515110227, 2021B1212040003), and by the State Key Laboratory of Subtropical Building Science at the South China University of Technology (as project 2021ZB12, 2022KA04, 2022KB15).

Data Availability Statement: The data presented in this study are available on request from the corresponding author. The data are not publicly available due to privacy.

Conflicts of Interest: The authors declare no conflict of interest.

Nomenclature

d	inner diameter of a brace
D	external diameter of a brace
w_{cf}	width of the column's flanges
$h_{cw}t_{cw}$	cross-sectional area of column's webs
M_{pb}	beam's plastic bending yield strength
W_{pb}	beam's plastic section modulus
f_y	steel's yield strength
M_{bry}	brace's bending yield strength
M_{pbc}	beam's plastic yield strength with the influence of two brace (top floor)
A_b	beam's cross-sectional area
L	beam's length
P	axial force applied by (circular steel tube) braces when they yield
A_{bry}	brace's cross-sectional area
q	uniform load on the beam based on η
η	axial compression ratio of braces

α	angle between beam and brace.
M'_{pbc}	beam's plastic yield strength with the influence of four brace (typical floor)
F_{br}	axial force applied by the upper braces at yielding
M_{cy}	bending yield strength of a column panel-zone
h_{bw}	height of the beam's web
h_{cw}	height of the column's web
t_{cw}	thickness of the column's web
λ	slenderness ratio of the braces
H	height of the structural floor
l_s	inner length of square tubular brace
L_s	external length of square tubular brace
L_{br}	brace's length
H_b	beam's height
B_b	beam's width
t_{bw}	beam's web thickness
t_{fw}	beam's flange thickness
t_{bry}	brace's thickness

Appendix A

Table A1. Finite element verification results (top floor, $\eta = 0.15, 0.2$ and 0.3).

Case	Column Section (mm)	Brace Section (mm)		Proposed Method	FEM Result
		External Diameters (η^1)	Thickness (η^1)		
13–15	HW 350 × 350 × 19 × 19	140 (0.15, 0.2, 0.3)	13 (0.15), 12 (0.2), 10 (0.3)	Brace Yielding	Brace Yielding
16–18	HW 344 × 348 × 10 × 16	140 (0.15, 0.2, 0.3)	13 (0.15), 12 (0.2), 10 (0.3)	Column Yielding before the beam	Column Yielding before the beam
19–21	HW 350 × 350 × 19 × 19	140 (0.15, 0.2, 0.3)	15 (0.15), 15 (0.2), 13 (0.3)	Beam Yielding	Beam Yielding
22–24	HW 350 × 350 × 19 × 19	140 (0.15, 0.2, 0.3)	8 (0.15, 0.2, 0.3)	Brace Yielding	Brace Yielding
25–27	HW 350 × 350 × 19 × 19	146 (0.15, 0.2), 144 (0.3)	16 (0.15), 15 (0.2), 12 (0.3)	Beam Yielding	Beam Yielding
28–30	HW 350 × 350 × 19 × 19	74 (0.15, 0.2, 0.3)	13 (0.15), 12 (0.2), 10 (0.3)	Brace Yielding	Brace Yielding

¹ η means the axial compression ratio of braces.

Table A2. Finite element verification results (typical floor, $\eta=0.15,0.2$ and 0.3).

Case	Column Section (mm)	Brace Section (mm)		Proposed Method	FEM Result
		External Diameters (η)	Thickness (η)		
31–33	HW 350 × 350 × 19 × 19	140 (0.2), 135 (0.15, 0.3)	10.5 (0.15), 10 (0.2), 9.5 (0.3)	Brace Yielding	Brace Yielding
34–36	HW 344 × 348 × 10 × 16	140 (0.2), 135 (0.15, 0.3)	10.5 (0.15), 10 (0.2), 9.5 (0.3)	Column Yielding before the beam	Column Yielding before the beam
37–39	HW 350 × 350 × 19 × 19	140 (0.2), 135 (0.15, 0.3)	13.5 (0.15), 13 (0.2), 10.5 (0.3)	Beam Yielding	Beam Yielding
40–42	HW 350 × 350 × 19 × 19	140 (0, 0.2), 135 (0.15, 0.3)	8 (0.2), 4.5 (0.15, 0.3)	Brace Yielding	Brace Yielding
43–45	HW 350 × 350 × 19 × 19	144 (0.15, 0.2), 142 (0.3)	15 (0.15), 12 (0.2), 13 (0.3)	Beam Yielding	Beam Yielding
46–48	HW 350 × 350 × 19 × 19	74 (0.15, 0.2, 0.3)	10.5 (0.15), 10 (0.2), 9.5 (0.3)	Brace Yielding	Brace Yielding

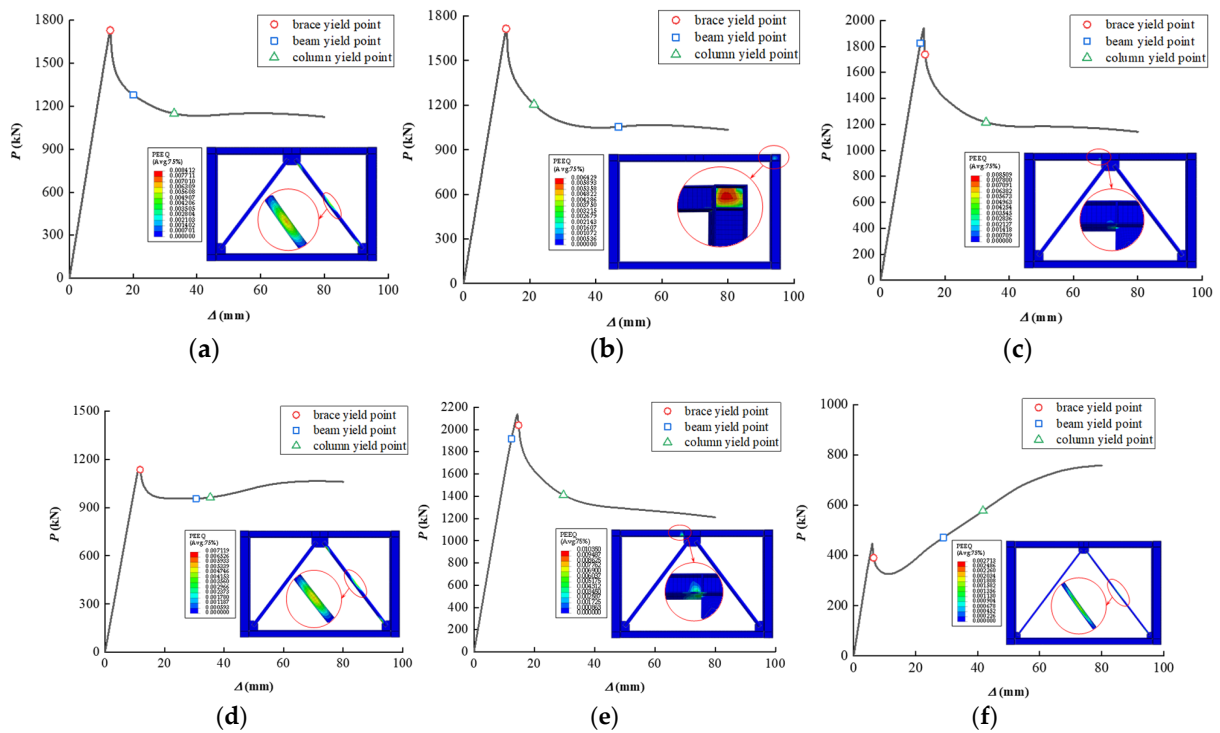


Figure A1. The predicted PEEQ distributions of top floor concentrically-braced steel frames ($\eta = 0.15$). (a) case 13, the basic model obtained by the proposed method; (b) case 16, smaller section area of column web; (c) case 19, thicker braces; (d) case 22, thinner braces; (e) case 25, larger brace external diameter than in the basic model; (f) case 28, smaller external diameter.

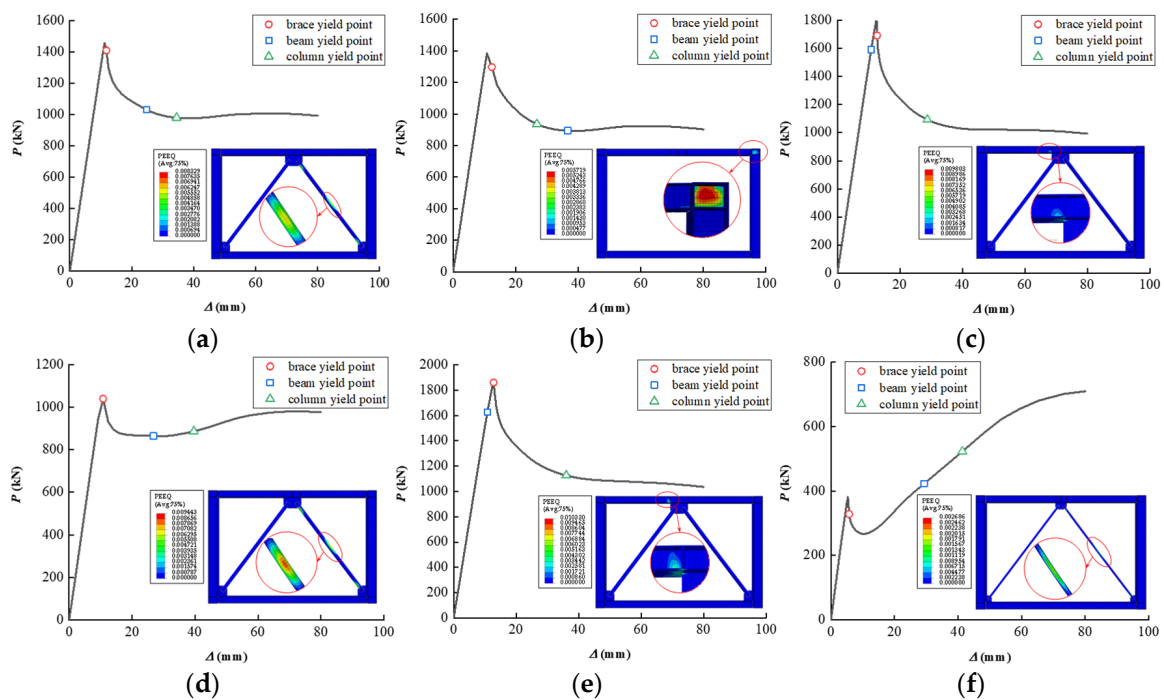


Figure A2. The predicted PEEQ distributions of top floor concentrically-braced steel frames ($\eta = 0.2$). (a) case 14, the basic model obtained by the proposed method; (b) case 17, smaller section area of column web; (c) case 20, thicker braces; (d) case 23, thinner braces; (e) case 26, larger brace external diameter than in the basic model; (f) case 29, smaller external diameter.

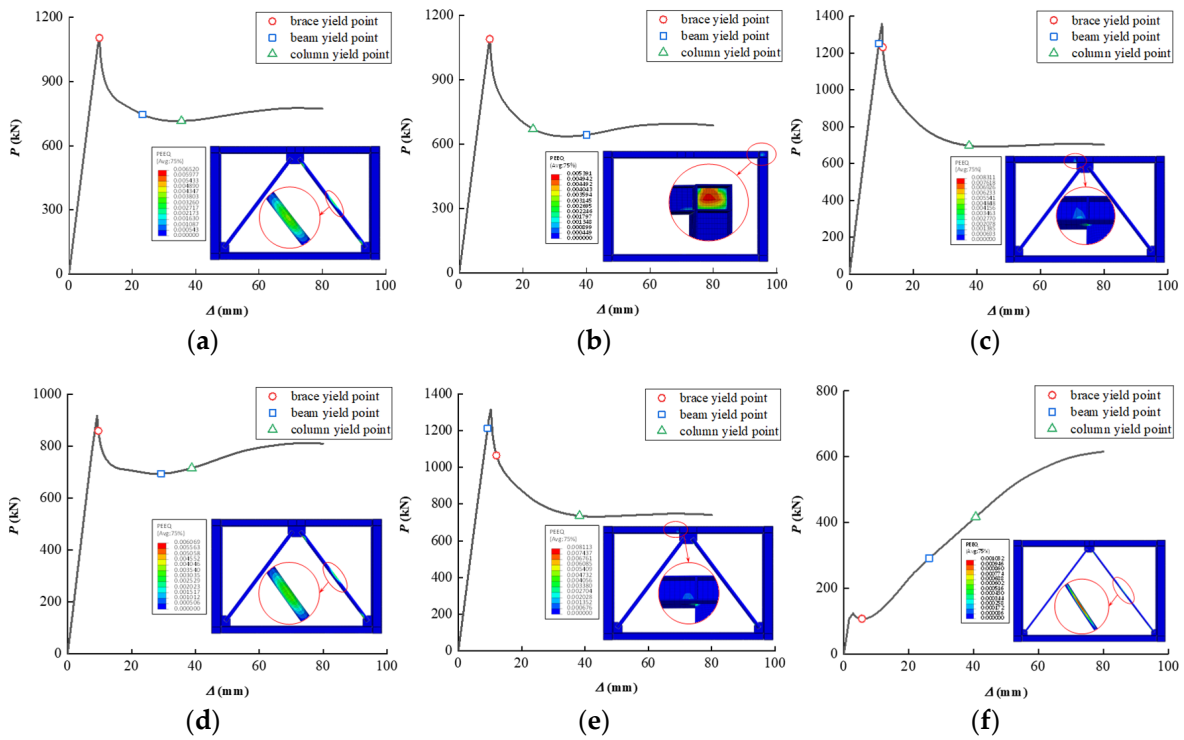


Figure A3. The predicted PEEQ distributions of top floor concentrically-braced steel frames ($\eta = 0.3$). (a) case 15, the basic model obtained by the proposed method; (b) case 18, with smaller column web section area; (c) case 20, thicker braces; (d) case 24, thinner braces than in the basic model; (e) case 27, larger external brace diameter; (f) case 30, smaller external brace diameter than in the basic model.

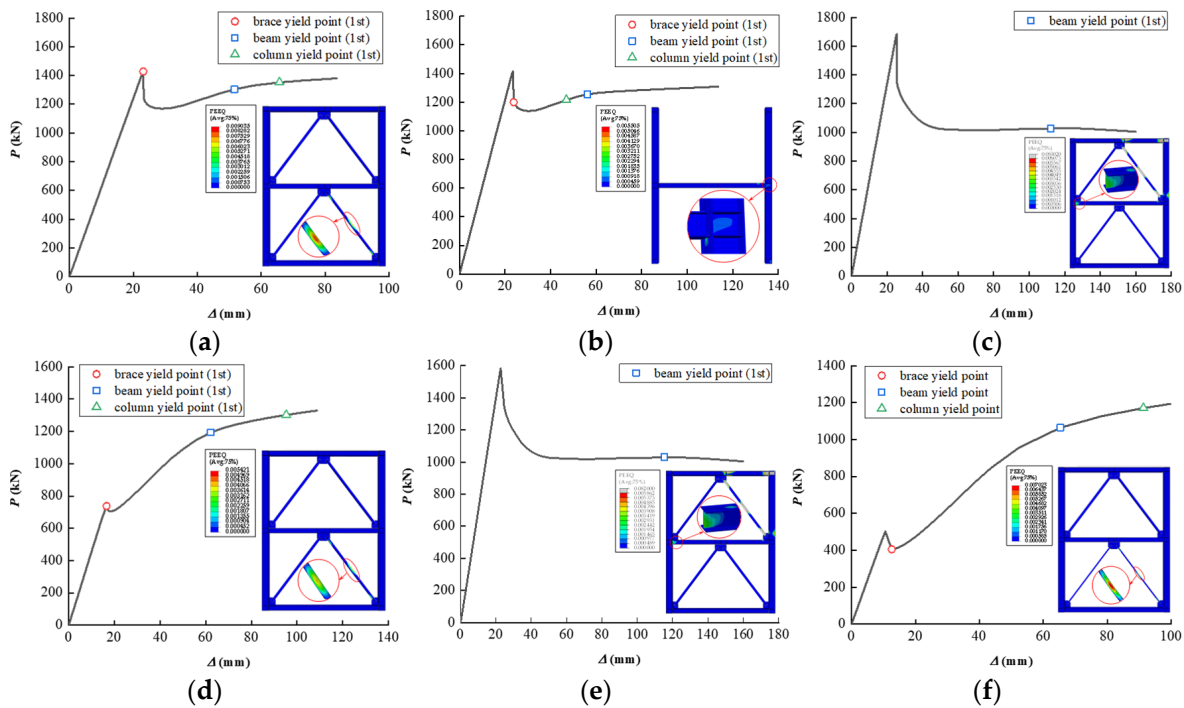


Figure A4. The predicted PEEQ distributions of a typical floor with $\eta = 0.15$. (a) case 31, the basic model obtained by the proposed method; (b) case 34, decreasing the section area of the column web; (c) case 37, thicker braces; (d) case 40, thinner braces; (e) case 43, larger brace external diameter; (f) case 46, smaller brace external diameter.

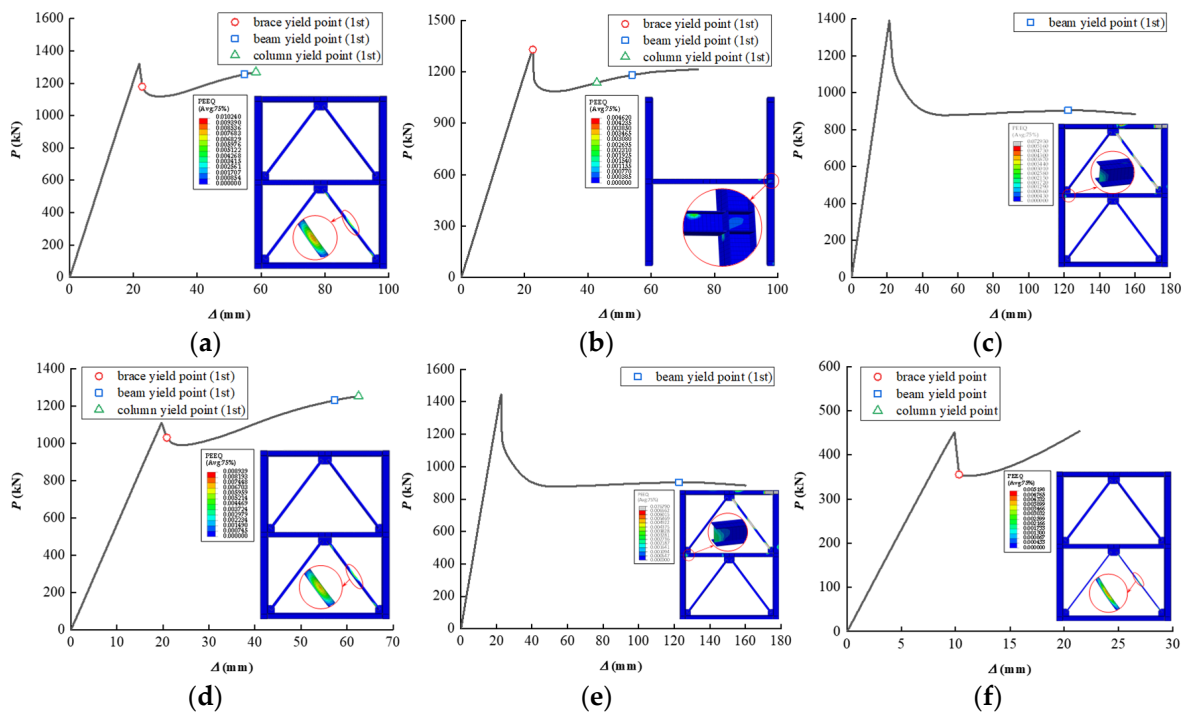


Figure A5. The predicted PEEQ distributions of a typical floor with $\eta = 0.2$. (a) case 32, the basic model obtained by the proposed method; (b) case 35, decreased section area of the column web; (c) case 38, thicker braces; (d) case 41, thinner braces; (e) case 44, larger external brace diameter; (f) case 47, smaller external brace diameter.

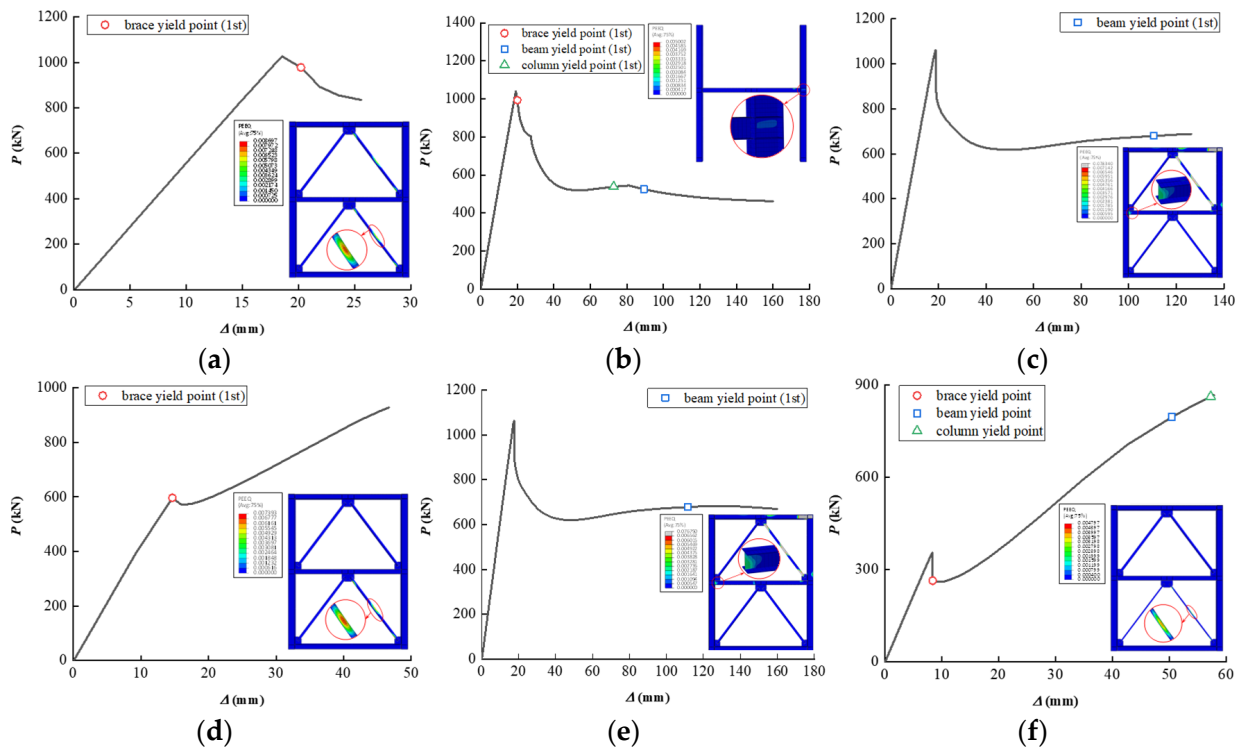


Figure A6. The predicted PEEQ distributions of a typical floor with $\eta = 0.3$. (a) case 33, the basic model obtained by the proposed method; (b) case 36, smaller column web section area; (c) case 39, thicker braces; (d) case 42, thinner braces; (e) case 45, larger external brace diameter; (f) case 48, smaller external brace diameter than in the basic model.

References

1. Costanzo, S.; Tartaglia, R.; Lorenzo, G.D.; Martino, A.D. Seismic Behaviour of EC8-Compliant Moment Resisting and Concentrically Braced Frames. *Buildings* **2021**, *9*, 196. [[CrossRef](#)]
2. Anonymous. *Code for Seismic Design of Buildings*; China Architecture & Building Press: Beijing, China, 2010.
3. Anonymous. *Standard for Design of Steel Structures*; China Architecture & Building Press: Beijing, China, 2017.
4. Anonymous. *Eurocode 8: Design of Structure for Earthquake Resistance*; British Standards Institution: London, UK, 2005.
5. Anonymous. *Seismic Provision of Structural Steel Buildings*; American Institute of Steel Construction: Chicago, IL, USA, 2016.
6. Tong, G.S.; Mi, X.F. Aseismic Behavior of Multistory Frames Based on Different Braces Design Methods. *Eng. Mech.* **2008**, *25*, 107–115.
7. Kumar, P.C.A.; Sahoo, D.R. Optimum Range of Slenderness Ratio of Hollow Steel Square Braces for Special Concentrically Braced Frames. *Adv. Struct. Eng.* **2016**, *19*, 928–944. [[CrossRef](#)]
8. Naderpour, M.N.; Aghakouchak, A.A. Probabilistic Damage Assessment of Concentrically Braced Frames with Built Up Braces. *J. Construct. Steel Res.* **2018**, *147*, 191–202. [[CrossRef](#)]
9. Kumar, P.C.A.; Sahoo, D.R. Fracture Ductility of Hollow Circular and Square Steel Braces under Cyclic Loading. *Thin-Wall Struct.* **2018**, *130*, 347–361. [[CrossRef](#)]
10. Sen, A.D.; Sloat, D.; Ballard, R.; Johnson, M.M.; Roeder, C.W.; Lehman, D.E.; Berman, J.W. Experimental Investigation of Chevron Concentrically Braced Frames with Yielding Beams. *J. Struct. Eng.* **2016**, *142*, 04016123. [[CrossRef](#)]
11. Leelataviwat, S.; Goel, S.C.; Stojadinovic, B. Energy-Based Seismic Design of Structures Using Yield Mechanism and Target Drift. *J. Struct. Eng.* **2002**, *128*, 1046. [[CrossRef](#)]
12. Sepahvand, M.F.; Akbari, J.; Kusunoki, K. Plastic Design of moment resisting frames using mechanism control. *J. Constr. Steel Res.* **2019**, *153*, 275–285. [[CrossRef](#)]
13. Sepahvand, M.F.; Akbari, J.; Kusunoki, K. Optimum Plastic Design of Moment Resisting Frames Using Mechanism Control. *Structures* **2018**, *16*, 254–268. [[CrossRef](#)]
14. Sepahvand, M.F.; Akbari, J. Toward Seismic Design of Tall Steel Moment Resisting Frames Using the Theory of Plastic Mechanism Control. *J. Build. Eng.* **2018**, *24*, 100705. [[CrossRef](#)]
15. Bai, J.L.; Ou, J.P. Seismic Plastic Limit-state Design of Frame Structures Based on the Strong-column Weak-beam Failure Mechanism. In Proceedings of the 15-WCEE, Lisbon, Portugal, 24–28 September 2012.
16. Mastrandrea, L.; Piluso, V. Plastic Design of Eccentrically Braced Frames, II: Failure Mode Control. *J. Constr. Steel Res.* **2008**, *65*, 1015–1028. [[CrossRef](#)]
17. Longo, A.; Montuori, R.; Piluso, V. Failure Mode Control of X-braced Frames Under Seismic Actions. *J. Earthq. Eng.* **2008**, *12*, 728–759. [[CrossRef](#)]
18. Longo, A.; Montuori, R.; Piluso, V. Plastic Design of Seismic Resistant V-braced Frames. *J. Earthq. Eng.* **2008**, *12*, 1246–1266. [[CrossRef](#)]
19. Mazzolani, M.F.; Piluso, V. Plastic Design of Seismic Resistant Steel Frames. *Earthq. Eng. Struct. Dyn.* **1997**, *26*, 167–191. [[CrossRef](#)]
20. Roeder, C.W.; Lehman, D.E.; Yoo, J.H. Improved Seismic Design of Steel Frame Connections. *Int. J. Steel Struct.* **2005**, *5*, 141–153.
21. Yang, R.Q.; Zhou, X.J. Low-cyclic Reversed Loading Tests of Chevron Concentrically Braced Steel Frames with Semi-rigid Connections of Different Details. *Prog. Steel Build. Struct.* **2021**, *23*, 75–84. [[CrossRef](#)]
22. Lai, J.W. Experimental and Analytical Studies on the Seismic Behavior of Conventional and Hybrid Braced Frames. Ph.D. Thesis, University of California, Berkeley, CA, USA, 2012.
23. Roeder, C.W.; Sen, A.D.; Terpstra, C.; Ibarra, S.M.; Liu, R.Y.; Lehman, D.E.; Berman, J.W. Effect of Beam Yielding on Chevron Braced Frames. *J. Constr. Steel Res.* **2019**, *159*, 428–441. [[CrossRef](#)]
24. Xu, J.; Wang, Z.; Wang, P.; Pan, J.R.; Li, B. Numerical Investigations on Large Size Stiffened Angle Connections with Different Bolt Patterns. *J. Construct. Steel Res.* **2021**, *182*, 106670. [[CrossRef](#)]
25. Yang, J.F.; Gu, Q.; Wan, H.; Peng, Y.L. Research on Pushover Test of Inverted-V Concentrically Braced Steel Frame. *J. Xi'an Univ. Archit. Technol. Nat. Sci. Ed.* **2010**, *5*, 656–662. [[CrossRef](#)]